RESEARCH PAPER

Poly ethylene oxide (PEO)–LiI polymer electrolytes embedded with CdO nanoparticles

A. Karmakar · A. Ghosh

Abstract Improvement of electrical conductivity of poly ethylene oxide (PEO)–LiI polymer electrolytes is necessary for their use in solid state lithium ion battery. In this study a new kind of PEO–LiI-based polymer electrolytes embedded with CdO nanoparticles with improved electrical conductivity has been prepared and characterized. The electron microscopic studies confirm that CdO nanoparticles of average size 2.5 nm are dispersed in the PEO matrix. The glass transition temperature of the PEO–LiI electrolyte decreases with the introduction of CdO nanoparticle in the polymer matrix. X-ray diffraction, electron microscopic, and differential scanning calorimetry studies show that the amorphous phase of PEO increases with the introduction of CdO nanoparticle and that the increase in amorphous phase is maximum for 0.10 wt% CdO doping. The electrical conductivity of the sample with 0.10 wt% CdO increases by three orders in magnitude than that of the PEO–LiI electrolyte. The electrical conductivity of PEO–LiI electrolyte embedded with CdO nanoparticle exhibits VTF behavior with reciprocal temperature indicating a strong coupling between the ionic and the polymer chain segmental motions.

Introduction

Ion conducting polymer electrolytes have drawn much attention because of their high energy density, good flexibility, mechanical strength, good cyclability, etc., for use as electrolytes in solid state lithium ion rechargeable batteries (Scrosati et al. 2001; Tarascon and Armand 2001; Dias et al. 2000). Mainly poly ethylene oxide (PEO)–lithium salt-based polymer electrolytes (Croce et al. 1998; Meyer 1998; Xi and Tang 2004; Gadjourova et al. 2001; Stoeva et al. 2003) have been studied extensively and the ionic conductivity is the key parameter of their performance. The dissolution of lithium salt in PEO electrolyte is due to the fact that PEO chains coil around the Li^+ ions and thus separates the cations from the counter anions (Dias et al. 2000). It is well established (Mao et al. 2000) that at room temperature the nature of PEO is biphasic containing both crystalline and amorphous phases and the transport of Li^+ cations in the polymer matrix is related to the local relaxation and segmental motion of PEO chains. These two mechanisms are achieved when the amorphous phase of PEO is dominant. Generally PEO tends to crystallize below its melting temperature (mp 60 °C) and thus shows much higher

A. Karmakar · A. Ghosh (✉)
Department of Solid State Physics, Indian Association for the Cultivation of Science, Jadavpur, Kolkata 700032, India
e-mail: sspag@iacs.res.in

crystalline phases near room temperature and the conductivity of these electrolytes is much lower than 10^{-5} Ω^{-1} cm^{-1}, which restricts its application in rechargeable batteries.

Over the last two decades, many efforts have been made to increase the conductivity of these polymer electrolytes. The addition of various plasticizers, such as tetraethylene glycol (TEG), ethylene carbonate (EC), propylene carbonate (PC) etc., to the polymer matrix increases their conductivity considerably (Frech and Chintapalli 1996; Kim and Smotkin 2002). However, they suffer from several drawbacks, such as decomposition, volatilization, reaction toward lithium metal electrode and also the deterioration of the mechanical properties. The addition of ceramic nanoparticles like Al_2O_3, TiO_2 in PEO–$LiClO_4$ electrolyte (Croce et al. 1998, 1999, 2001) and inclusion of inorganic nanoparticles as fillers in the PEO–lithium salt-based polymer electrolytes (Wang et al. 2009; Bhattacharya and Ghosh 2008; Fan et al. 2003; Ribeiro et al. 2001; Scrosati et al. 2000; Nan et al. 2003) improves the conductivity considerably but below 10^{-4} Ω^{-1} cm^{-1}.

In this study synthesis of PEO–LiI polymer nancomposite electrolyte embedded with different concentrations of CdO nanoparticles of average size 2.5 nm has been reported. It has been observed that the increase of amorphous phase of PEO–LiI electrolytes and hence the electrical conductivity is maximum for 0.10 wt% CdO doping concentration.

Experimental

First, CdO nanoparticle was synthesized by dissolving cadmium chloride ($CdCl_2$) in distilled water and then adding NaOH bead into the solution under stirring condition. A white precipitation of $Cd(OH)_2$ was produced. Then it was filtered and washed for several times to remove the insoluble residue to find $Cd(OH)_2$ colloid. It was then heat treated at 400 °C for 24 h to obtain the CdO nanoparticles powder.

To prepare PEO–LiI electrolyte, PEO (MW = 400000, Aldrich) and appropriate amount of vacuum dried anhydrous LiI (Aldrich) were dissolved together in acetonitrile. The molar ratio of the ethylene oxide segments to the lithium ions was maintained at [EO]/[Li] = 12. After stirring for 24 h at room temperature, the solutions became very thick after solvent evaporation. Then it was cast in PTFE containers and dried in

a vacuum oven at 55 °C for 36 h to form the free standing homogeneous films of about 0.01 cm thick.

Finally, the PEO–LiI-x wt% CdO nanocomposite electrolytes were prepared by dissolving appropriate amount of PEO and vacuum dried anhydrous LiI together in acetonitrile. The molar ratio of the ethylene oxide segments to the lithium ions was kept same as stated above. Then different concentrations of CdO nanoparticles ($x = 0.05$–0.20 wt%) were dispersed in acetonitrile separately and added into the mixture under stirring condition. After stirring for 24 h at room temperature, the solutions became very thick and free standing homogeneous films were produced following the same procedure as for PEO–LiI electrolytes as stated above.

X-ray diffraction (XRD) pattern of the CdO powder, as-prepared PEO–LiI films and PEO–LiI–CdO nanocomposite films were recorded in an X-ray diffractometer (D8 ADVANCE, BRUKER AXS) using CuK$_\alpha$ radiation (0.154 nm wavelength) at a scan rate of 1 degree min^{-1}. The differential scanning calorimetry (DSC) experiments were performed at a heating scan rate of 10 °C min^{-1} in Perkin-Elmer DSC-7 in N_2 atmosphere. The samples were mounted on a specimen stub and coated with platinum and a JSM-6700F field emission scanning electron microscope (FE-SEM) (JEOL Co.), equipped with a link elemental analyzer and a silicon detector, was used for studying the surface morphology of the films. For transmission electron microscopic (TEM) studies a few drops of gel samples just before casting were sonicated in acetonitrile for 15 min in an ultrasonic bath (EYELA) and were dropped in a 300 mesh copper grid. The TEM images were taken using a high resolution TEM (HR-TEM, JEOL, model JEM 2010). Ionic conductivity of the PEO–LiI and PEO–LiI–CdO films were determined at various temperatures by ac impedance spectroscopy in the anhydrous environment in the frequency range 10 Hz–2 MHz using a RLC meter (QuadTech, model 7600). A conductivity cell containing two stainless steel blocking electrodes was used for the ac impedance measurement.

Results and discussion

Figure 1a shows the XRD pattern of CdO powder. A perfect match of the diffraction peaks with those from
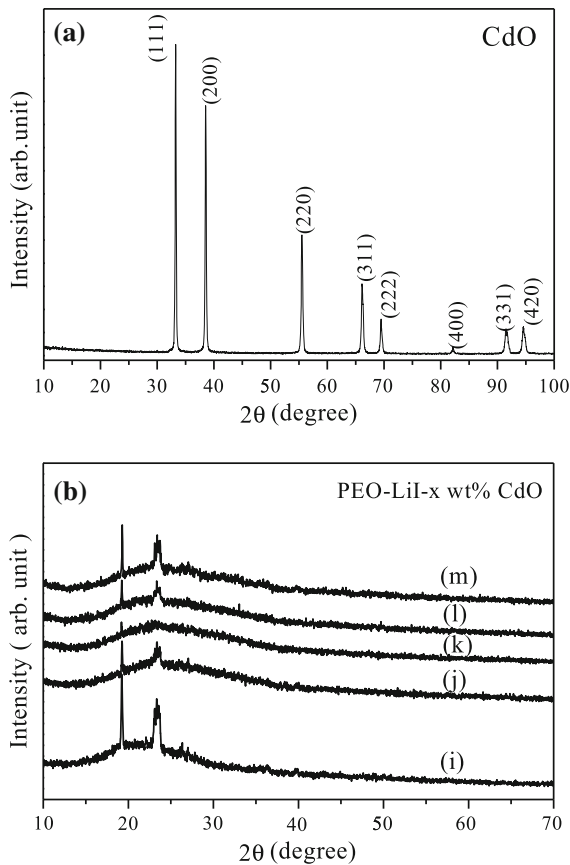
Fig. 1 **a** XRD pattern for CdO powder. **b** XRD patterns for PEO–LiI-*x* wt% CdO polymer electrolytes: (*i*) for *x* = 0; (*j*) for *x* = 0.05; (*k*) for *x* = 0.10; (*l*) for *x* = 0.15, and (*m*) for *x* = 0.20

JCPDS datasheet (JCPDS Datasheet No. 05-0640) indicates the absence of any impurity. The XRD patterns of the as-prepared PEO–LiI and PEO–LiI-*x* wt% CdO nanocomposite electrolytes are shown in Fig. 1b. No characteristic peaks for LiI have been observed in Fig. 1b, indicating that LiI forms complex with the ether oxygen of PEO (Wang et al. 2006). Two diffraction peaks (at $2\theta = 19°$ and $23.5°$) are observed for PEO–LiI electrolyte which are the characteristic peaks of PEO due to its crystalline phase. Figure 1b clearly indicates that the PEO–LiI electrolyte shows highest peak intensity, suggesting highest crystalline phase of PEO. With the addition of CdO in the PEO–LiI matrix, the peak intensity of crystalline PEO decreases and only trace of crystalline PEO has been detected for 0.10 wt% CdO nanoparticles in the PEO–LiI matrix, indicating that significant reduction in the crystalline phase of PEO
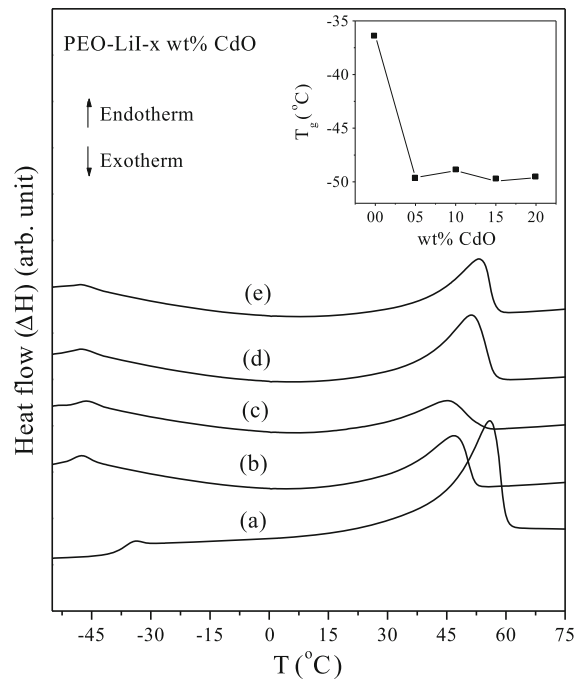

Fig. 2 DSC thermograms for PEO–LiI-*x* wt% CdO polymer electrolytes: (*a*) for *x* = 0; (*b*) for *x* = 0.05; (*c*) for *x* = 0.10; (*d*) for *x* = 0.15, and (*e*) for *x* = 0.20. *Inset* shows the variation of glass transition temperature (T_g) with CdO concentration

and a homogeneous electrolyte with a high degree of dispersion of the CdO occurs for this composition. When the concentration of CdO is increased beyond the optimum value of 0.10 wt% the intensity of the two peaks tends to increase again, showing the increase of crystalline phase of PEO.

The DSC traces of PEO–LiI and PEO–LiI-*x* wt% CdO nanocomposite electrolytes are displayed in Fig. 2. The thermodynamic parameters such as glass transition temperature (T_g), melting temperature (T_m), and melting enthalpy (ΔH_m) were obtained from the DSC traces and are summarized in Table 1. The percentage of crystalline phase of PEO (X_c) has been calculated using the equation

$$X_c = \Delta H_m / \Delta H_{PEO}, \tag{1}$$

where ΔH_m is the melting enthalpy of the sample and ΔH_{PEO} is the melting enthalpy (namely 213.7 J g^{-1}) of completely crystallized PEO (Li and Hsu 1984). The inset of Fig. 2 shows the variation of T_g with CdO doping concentration. It can be observed that when CdO nanoparticles is doped into PEO–LiI polymer electrolyte the glass transition temperature

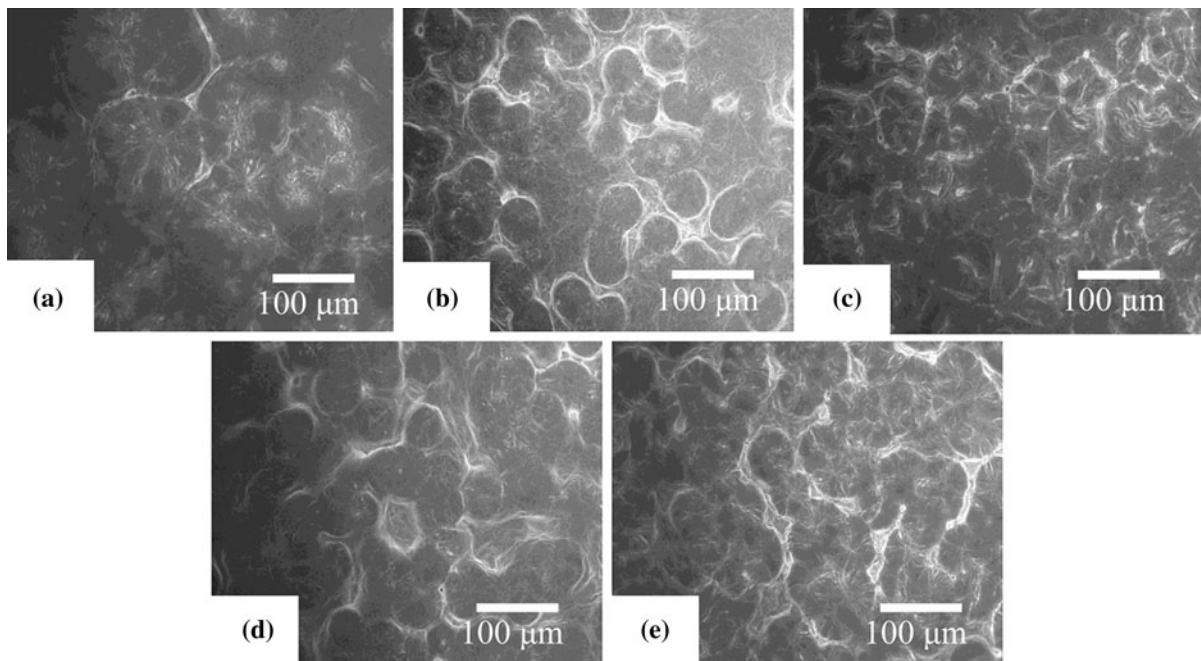**Table 1** Comparison of thermal parameters of PEO–LiI–CdO nanocomposite electrolytes obtained from DSC

Wt% CdO	T_g (°C) (±2)	T_m (°C) (±2)	ΔH (J g^{-1})	X_c (%)
0	−36.4	55.9	51.9	24.3
0.05	−49.6	46.8	28.8	13.4
0.10	−48.9	45.1	25.3	11.8
0.15	−49.9	51.2	39.3	18.4
0.20	−49.6	53.2	41.0	19.2

T_g decreases from −36.4 °C to around −49 °C and does not change considerably with doping concentration. This result suggests improvement in the flexibility of the polymer host backbone. It is noted in Table 1 that the values of T_m and ΔH_m for all concentrations of CdO are lower than that for PEO–LiI electrolytes with lowest values for 0.10 wt%. A lower ΔH_m value shows a reduced degree of crystalline phase. This decrease in crystallinity of PEO is due to the fact that the introduction of CdO nanoparticles lowers the reorganization tendency of polymer chain via the interaction with Li$^+$ and PEO, promoting amorphous regions and leading to the formation of an amorphous interface area surrounding the nanoparticles (Croce et al. 1998; Nan et al.

2003). The lowest value of X_c (11.8%) achieved for 0.10 wt% CdO suggests the formation of good complexation with a large ratio of amorphous phase to crystalline phase.

Figure 3 shows the FE-SEM micrographs of PEO–LiI and PEO–LiI–CdO nanocomposite electrolytes for varying concentration of CdO nanoparticle. The electrolytes exhibit a spherulite like surface structure, which is a typical morphology of a crystalline PEO with flexible chains. The amorphous phase of PEO is also observed in the gap between spherulites. The small pores are caused by the fast evaporation of the acetonitrile solvent during the preparation process.

The average size (diameter) of spherulites for PEO–LiI electrolytes (Fig. 3a) is found to be 120 μm. Also the spaces in between the spherulites i.e., the amorphous regions of PEO in this electrolyte are very narrow. It is interesting to note that when CdO is inserted into PEO–LiI electrolyte the number of PEO spherulites increases and the average size of spherulites decreases to about 50 μm (Fig. 3b–e), which are both beneficial for the decreasing of the crystalline phase of PEO (Xi et al. 2005, 2006). CdO acts as a nucleation site of spherulite and provides an obstacle for the spherulite growth (Jeong et al. 2007). It is

Fig. 3 FE-SEM images of polymer electrolyte films of PEO–LiI-x wt% CdO: **a** for $x = 0$; **b** for $x = 0.05$; **c** for $x = 0.10$; **d** for $x = 0.15$, and **e** for $x = 0.20$

observed that the size of the spherulites does not change appreciably with the variation of CdO concentration, but the change of amorphous phase between spherulites is significant. A dramatic improvement of the amorphous phase of PEO is observed when 0.10 wt% CdO is doped into the matrix (Fig. 3c). However, further increase of CdO content decrease the amorphous region between the spherulites. The increased amount of amorphous phase in between the spherulites is very much important for conduction of Li$^+$ ions.
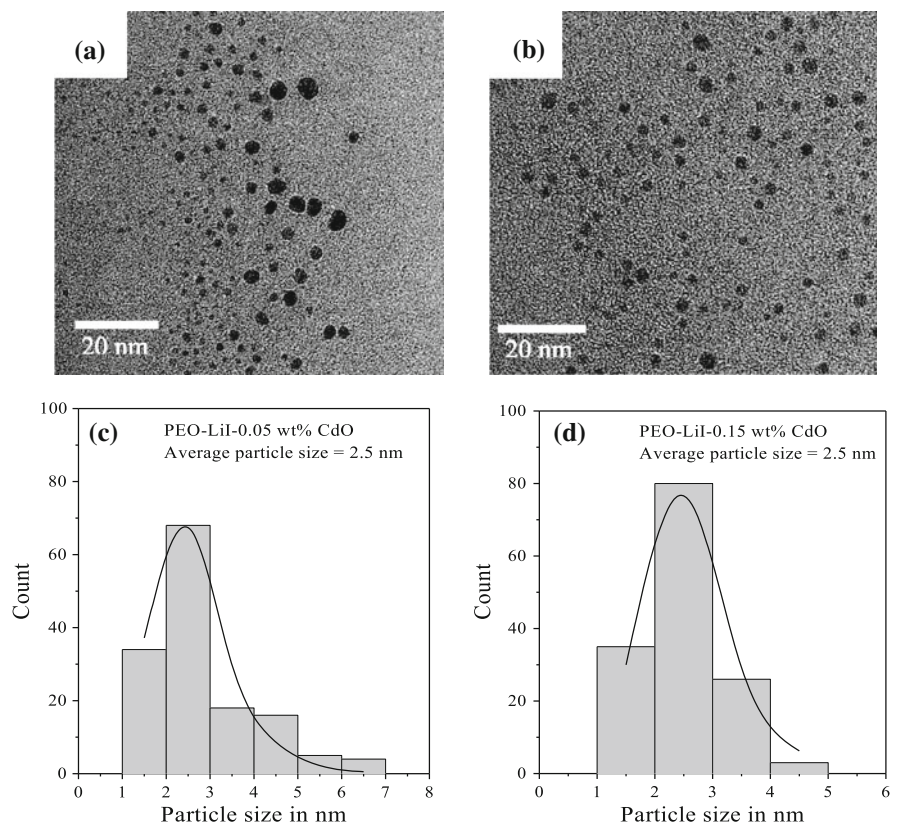
The transmission electron micrographs for the two samples of PEO–LiI–CdO nanocomposite electrolytes with 0.05 and 0.10 wt% CdO are shown in Fig. 4a and b, respectively. The TEM images show that CdO nanoparticles are distributed in the polymer matrix. The histograms for the distribution of the particle size, calculated from TEM images, are shown in Fig. 4c and d, respectively, for these samples. The average size of the particles has been obtained from the fits of the data to the log normal distribution (Soderlund et al. 1998) given by the following relation

$$f(r) = \frac{1}{\sqrt{2\pi}\ln\sigma}\exp\left\{-\frac{(\ln r - \ln\rho)}{2(\ln\sigma)^2}\right\}, \qquad (2)$$

where r is particle diameter, ρ is the geometric mean diameter, and σ is the dimensionless geometric standard deviation. The average size of the particles obtained from the fits is 2.5 nm in both the cases. Similar distribution of particles has been observed with the same average particle size for other CdO contents.

Figure 5 shows the variation of the dc conductivity at $T = 303$ K, obtained from complex impedance plot, as a function of CdO concentration. The dc conductivity first increases sharply with the increase of CdO concentration and attains a maximum value for 0.10 wt% CdO and then decreases beyond this concentration. It may be noted that the dc conductivity (3×10^{-4} S cm^{-1}) for nanocomposite electrolyte with 0.10 wt% CdO is about three orders in magnitude higher than that of the PEO–LiI electrolyte. Basically, the ion transport in PEO–Li salt-based electrolyte occurs due to the movement of Li$^+$ ions

Fig. 4 TEM images of a PEO–LiI-0.05 wt% CdO polymer electrolytes and b PEO–LiI-0.15 wt% CdO polymer electrolytes. c and d are histograms for distribution of CdO nanoparticles shown for PEO–LiI-0.05 wt% CdO polymer electrolytes and PEO–LiI-0.15 wt% CdO polymer electrolytes, respectively. The *solid curves* are the fits to lognormal function (Eq. 2)
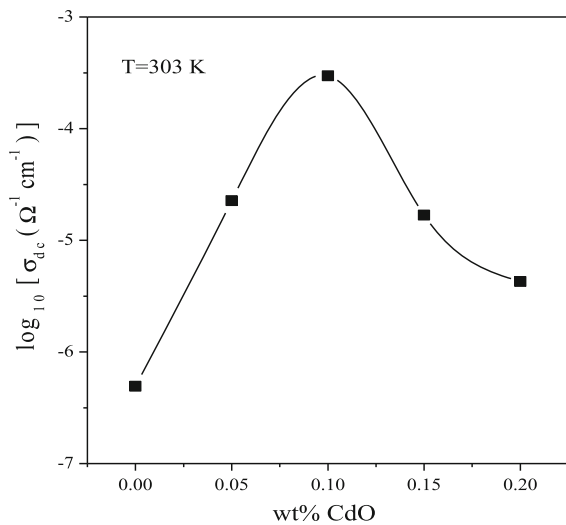
Fig. 5 Variation of dc conductivity for PEO–LiI-x wt% CdO polymer electrolytes with CdO concentration at $T = 303$ K

through the amorphous phase of PEO (Croce et al. 1998, 1999; Xi and Tang 2004). For the present PEO–LiI–CdO, XRD, SEM, and DSC studies show that when 0.10 wt% CdO nanoparticles is doped into the PEO–LiI matrix the amorphous phase of PEO attains its maximum value. For the present compositions the incremental amorphous phase increases the movement of Li$^+$ ions through the matrix which in turn increases the dc conductivity and the highest conductivity of the composition with 0.10 wt% of CdO is due to the maximum amorphous phase for this composition. The decrease in the conductivity for higher CdO concentration is attributed to the fact that at higher concentration of CdO, the aggregation of the nanoparticles takes place due to inter particle interaction which in turn provides a blockage on the transport of charge carriers (Wang et al. 2009; Fan et al. 2003; Nan et al. 2003; Kumar et al. 2001).

The variation of logarithmic electrical conductivity for all compositions with reciprocal temperature is shown in Fig. 6. An Arrhenius type of behavior is obtained for PEO–LiI electrolyte with activation energy of 1.98 eV. Other authors (Itho et al. 2003; Ramesh et al. 2002) also observed such type of behavior in polymeric system below melting point. But the conductivity variation of CdO-doped electrolytes has been well described by the Vogel–Tamman–Fulcher (VTF) relation (Vogel 1921; Tamman and Hesse 1926; Fulcher 1925) expressed as
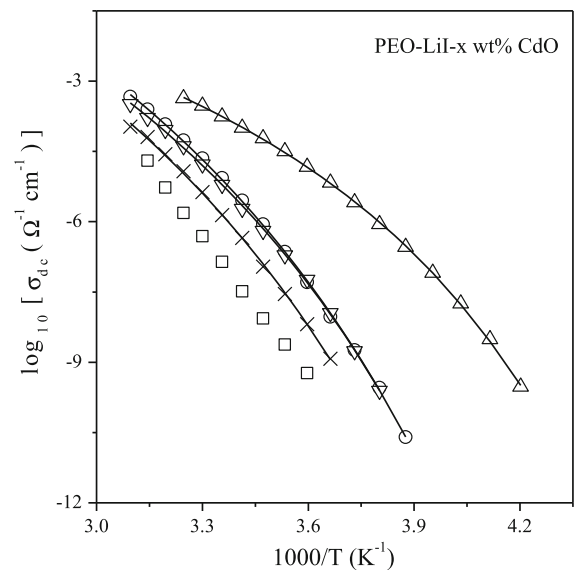

Fig. 6 Variation of dc conductivity with reciprocal temperature of PEO–LiI-x wt% CdO polymer electrolytes: *square* for $x = 0$; *circle* for $x = 0.05$; *triangle* for $x = 0.10$; *inverted triangle* for $x = 0.15$, and *times symbol* for $x = 0.20$. The *solid lines* are the VTF fits (Eq. 3)

Table 2 The VTF fitting parameters obtained for of PEO–LiI–CdO nanocomposite electrolytes

Wt% CdO	Log(σ_0) (Ω^{-1} cm^{-1})	E_a (eV) (± 0.002)	T_0 (°C) (± 2)
0.05	6.32	0.043	−89
0.10	2.54	0.021	−88
0.15	5.58	0.040	−86
0.20	6.16	0.045	−87

$$\sigma = \sigma_0 T^{-1/2} \exp\left[\frac{-E_a}{k_B(T - T_0)}\right], \qquad (3)$$

where σ_0 is the conductivity pre-exponential factor, k_B is the Boltzman constant, E_a is the Vogel activation energy, T_0 is the Vogel scaling temperature, and T is the absolute temperature. The conductivity data for the CdO-doped electrolytes were fitted to Eq. 3 using non linear least square fits. The fitting parameters σ_0, E_a, and T_0 are shown in Table 2. Generally, the value of ($T_g - T_0$) is of the order of 50 K for polymeric system (Angell 1983; Natesan et al. 2006). The values of T_0 obtained from the fit are about 40 K lower than the values of T_g. The VTF

model proposes that the ionic conductivity is favored as a result of the segmental motion of the polymer chain in the matrix. A reasonably good fit of the conductivity to VTF relation over a wide range of temperature clearly indicates that a strong coupling exists between the ionic and the polymer chain segmental motions of the investigated CdO-doped electrolytes (Ribeiro et al. 2001; Fragiadakis et al. 2008).

Conclusions

In this study, novel PEO–LiI polymer nanocomposite electrolyte embedded with CdO nanoparticles with improved electrical conductivity has been synthesized. CdO nanoparticles of average size 2.5 nm have been prepared by thermal route. For a doping concentration of 0.10 wt% CdO into the PEO–LiI matrix, the increase of amorphous phase of PEO is maximum. At this doping level the nanocomposite electrolyte forms a good complexion and a significant enhancement of the dc conductivity has been observed. However, beyond this concentration the conductivity decreases due to blocking effect on the transport of ions resulting from aggregation of nanoparticles. The temperature dependence of the dc conductivity of the CdO-doped electrolytes is well explained by the VTF relation.

References

Angell CA (1983) Fast ion motion in glassy and amorphous materials. Solid State Ionics 9–10:3–16

Bhattacharya S, Ghosh A (2008) Effect of ZnO nanoparticles on the structure and ionic relaxation of poly(ethylene oxide)–LiI polymer electrolyte nanocomposites. J Nanosci Nanotech 8:1922–1926

Croce F, Appetecchi GB, Persi L, Scrosati B (1998) Nanocomposite polymer electrolytes for lithium batteries. Nature 394:456–458

Croce F, Curini R, Martinelli A, Persi L, Ronci F, Scrosati B (1999) Physical and chemical properties of nanocomposite polymer electrolytes. J Phys Chem B 103:10632–10638

Croce F, Persi L, Scrosati B, Fiory FS, Plichta E, Hendrickson MA (2001) Role of the ceramic fillers in enhancing the transport properties of composite polymer electrolytes. Electrchimica Acta 46:2457–2461

Dias FB, Plomp L, Veldhuis JBJ (2000) Trends in polymer electrolytes for secondary lithium batteries. J Power Sources 88:169–191

Fan L, Dang Z, Wei G, Nan CW, Li M (2003) Effect of nanosized ZnO on the electrical properties of $(PEO)_{16}LiClO_4$ electrolytes. Mater Sci Eng B 99:340–343

Fragiadakis D, Dou S, Colby RH, Runt J (2008) Molecular mobility, ion mobility, and mobile ion concentration in poly(ethylene oxide)-based polyurethane ionomers. Macromolecules 41:5723–5728

Frech R, Chintapalli S (1996) Effect of propylene carbonate as a plasticizer in high molecular weight $PEO-LiCF_3SO_3$ electrolytes. Solid State Ionics 85:61–66

Fulcher GS (1925) Analysis of recent measurements of the viscosity of glasses. J Am Ceram Soc 8:339–355

Gadjourova Z, Andreev YG, Tunstall DP, Bruce PG (2001) Ionic conductivity in crystalline polymer electrolytes. Nature 412:520–523

Itho T, Miyamura Y, Ichikawa Y, Uno T, Kubo M, Yamamoto O (2003) Composite polymer electrolytes of poly(ethylene oxide)/$BaTiO_3$/Li salt with hyperbranched polymer. J Power Sources 119–121:403–408

Jeong SS, Lim YT, Choi YJ, Cho GB, Kim KW, Ahn HJ, Cho KK (2007) Electrochemical properties of lithium sulfur cells using PEO polymer electrolytes prepared under three different mixing conditions. J Power Sources 174:745–750

Kim YT, Smotkin ES (2002) The effect of plasticizers on transport and electrochemical properties of PEO-based electrolytes for lithium rechargeable batteries. Solid State Ionics 149:29–37

Kumar B, Scanlon LG, Spry RJ (2001) On the origin of conductivity enhancement in polymer–ceramic composite electrolytes. J Power Sources 96:337–342

Li X, Hsu SL (1984) An analysis of the crystallization behavior of poly(ethylene oxide)/poly(methyl methacrylate) blends by spectroscopic and calorimetric techniques. J Polym Sci Polym Phys Ed 22:1331–1342

Mao G, Perea RF, Howells WS, Price DL, Saboungi ML (2000) Relaxation in polymer electrolytes on the nanosecond timescale. Nature 405:163–165

Meyer WH (1998) Polymer electrolytes for lithium-ion batteries. Adv Mater 10:439–448

Nan CW, Fan L, Lin Y, Cai Q (2003) Enhanced ionic conductivity of polymer electrolytes containing nanocomposite SiO_2 particles. Phys Rev Lett 91:266104

Natesan B, Karan NK, Katiyar RS (2006) Ion relaxation dynamics and nearly constant loss behavior in polymer electrolyte. Phys Rev E 74:042801

Ramesh S, Yahaya AH, Arof AK (2002) Dielectric behaviour of PVC-based polymer electrolytes. Solid State Ionics 152–153:291–294

Ribeiro R, Silva GG, Mohallen NDS (2001) A comparison of ionic conductivity, thermal behaviour and morphology in two polyether–LiI–$LiAl_5O_8$ composite polymer electrolytes. Electrchimica Acta 46:1679–1686

Scrosati B, Croce F, Persi L (2000) Impedance spectroscopy study of PEO-based nanocomposite polymer electrolytes. J Electrochem Soc 147:1718–1721

Scrosati B, Croce F, Panero S (2001) Progress in lithium polymer battery R&D. J Power Sources 100:93–100

Soderlund J, Kiss LB, Niklasson GA, Granqvist CG (1998) Lognormal size distributions in particle growth processes without coagulation. Phys Rev Lett 80:2386–2388

Stoeva Z, Litas IM, Staunton E, Andreev YG, Bruce PG (2003) Ionic conductivity in the crystalline polymer electrolytes PEO_6:$LiXF_6$, X = P, As, Sb. J Am Chem Soc 125:4619–4626

Tamman G, Hesse W (1926) The dependence of viscosity upon the temperature of supercooled liquids. Z Anorg Allg Chem 156:245–257

Tarascon JM, Armand M (2001) Issues and challenges facing rechargeable lithium batteries. Nature 414:359–367

Vogel H (1921) Temperature dependence of viscosity of melts. Z Phys 22:645–646

Wang YJ, Pan Y, Wang L, Pang MJ, Chen L (2006) Characterization of (PEO)$LiClO_4$-$Li_{1.3}Al_{0.3}Ti_{1.7}(PO_4)_3$ composite polymer electrolytes with different molecular weights of PEO. J Appl Poly Sci 102:4269–4275

Wang L, Yang W, Wang J, Evans DG (2009) New nanocomposite polymer electrolyte comprising nanosized $ZnAl_2O_4$ with a mesopore network and PEO–$LiClO_4$. Solid State Ionics 180:392–397

Xi J, Tang X (2004) Nanocomposite polymer electrolyte based on poly(ethylene oxide) and solid super acid for lithium polymer battery. Chem Phys Lett 393:271–276

Xi J, Qiu X, Zheng S, Tang X (2005) Nanocomposite polymer electrolyte comprising PEO/$LiClO_4$ and solid super acid: effect of sulphated-zirconia on the crystallization kinetics of PEO. Polymer 46:5702–5706

Xi J, Qiu X, Wang J, Bai Y, Zhu W, Chen L (2006) Effect of molecular sieves ZSM-5 on the crystallization behavior of PEO-based composite polymer electrolyte. J Power Sources 158:627–634